HOSTED BY

ELSEVIER

CrossMark

Available online at www.sciencedirect.com

ScienceDirect

Progress in Natural Science: Materials International 25 (2015) 179–184

Progress in Natural Science Materials International

www.elsevier.com/locate/pnsmi
www.sciencedirect.com

Original Research

Solvent-free selective hydrogenation of *o*-chloronitrobenzene to *o*-chloroaniline over alumina supported Pt nanoparticles

Qiang Bai, Dan Li, Lu He, Hailian Xiao, Ning Sui*, Manhong Liu*

College of Materials Science and Engineering, Qingdao University of Science and Technology, Qingdao 266042, China

Received 27 March 2014; accepted 16 October 2014
Available online 8 July 2015

Abstract

A supported Pt/Al_2O_3 catalyst was prepared by immobilizing preformed colloidal Pt nanoparticles on Al_2O_3. The particle size and size distribution of Pt particles on Al_2O_3 remained the same as the colloidal nanoparticles. Selective hydrogenation of *o*-chloronitrobenzene to *o*-chloroaniline was performed on the as-prepared Pt/Al_2O_3 nanocatalyst without using any solvent and 88.5% selectivity to *o*-chloroaniline at 98.2% conversion of *o*-chloronitrobenzene was achieved. Further catalytic experiments with metal cation modification showed that some metal cations could improve the activity in various degrees while maintaining the high selectivity. Especially, 99.8% selectivity to *o*-chloroaniline at ~100% conversion was attained with Sn^{4+}.

Keywords: Chloroaniline; Selective hydrogenation; Solvent-free; Nanoparticle; Metal cation modification

1. Introduction

Consideration of the principles of green chemistry, increasing attention has been paid to running reactions in an environment friendly and atom economic way. Solvent-free reaction is an effective method to reduce pollution, lower costs, save energy, and simplify purification procedures. Solvent-free conditions often lead to shorter reaction times, increased product yields, and easier workup. Scale-up is also facilitated by solvent-free techniques. Therefore, researchers have been working on solvent-free conditions for both the laboratory synthesis and the industrial manufacturing [1,2]. Some recent works on this direction include the Hantzsch reaction [3], the alkene hydrogenation reaction [4], the alcohol and aldehyde oxidation over Au/MgO [5], and the alkylation of amines with alcohols over organo-iridium catalysts [6].

Catalytic hydrogenation of chloronitrobenzenes to aromatic chloroamines is an important step in the production of many fine chemicals, such as dyes, drugs, herbicides, corrosion inhibitors, pharmaceuticals, cosmetic products, pesticides, and insecticides [7]. Various hydrogenation methods for nitroarenes with palladium [8], platinum [9,10], ruthenium [11], iridium [12], silver [13], and gold [14] have been studied. In order to improve the activity and selectivity, some strategies have been developed, including tuning the nature of the catalyst (new active metal [15], using second metal [16,17], varying metal particle size [18] and support [19]), introducing the additives (promoter, inhibitor, and poison) [20], and changing the reaction conditions (solvent, temperature, and pressure) [13,18].

Traditional supported catalysts are usually made by wet impregnation, i.e. the catalyst supports firstly adsorb the catalyst precursors dispersed in solvents, and then they are dried and undergo high temperature treatments such as H_2 gas reduction. In the preparation of the supported metal catalysts, a great concern is how to produce metal particles that are well dispersed with small sizes in order to maximize the surface-to-volume ratio [21,22]. The narrow particle size distribution is an important factor as well for the selectivity purpose [23]. However, impregnation is not easy to control the particle size and the size distribution, and catalysts prepared by traditional methods often exhibit poor reproducibility [24]. An alternate

*Corresponding authors. Tel./fax: +86 532 8402 2814.
E-mail addresses: suining1982@gmail.com (N. Sui), liumanhong68@126.com (M. Liu).

Peer review under responsibility of Chinese Materials Research Society.

http://dx.doi.org/10.1016/j.pnsc.2015.05.005

method to obtain supported catalysts with well-defined metal particles is to immobilize preformed nanoparticles on supports, such as the colloidal nanoparticles [25]. The great advantage of the colloidal nanoparticles is that the particle size, size distribution and the crystal structure of those nanoparticles can be well controlled. Various techniques to immobilize the preformed colloidal metal nanoparticles with controllable size and size distribution on supports have been investigated [26–28].

In this work, we made small Pt colloidal nanoparticles using ethylene glycol reduction and then immobilized them on alumina support (Pt/Al_2O_3). This supported nanocatalyst was used to selectively hydrogenate *o*-chloronitrobenzene (*o*-CNB) to *o*-chloroaniline (*o*-CAN) without solvent. We also investigated the metal cation modification effect on this reaction and found that some metal cations could improve the activity in various extents while maintaining the high selectivity. When using Sn^{4+} as the modifier, we obtained 99.8% selectivity to *o*-CAN at ~100% conversion of *o*-CNB.

2. Materials and methods

2.1. Materials

Hydrogen gas (H_2) with a purity of 99.999% was supplied from Beijing Gas Factory. *o*-CNB was re-crystallized in ethanol before use. Water was distilled and deionized before use. Hydrogen hexachloroplatinate (IV) hexahydrate ($H_2PtCl_6 \cdot 6H_2O$) and other reagents were of analytical grade purity and were used as received (Beijing Chemicals Co.).

2.2. Preparation of nearly monodisperse colloidal platinum nanoparticles

The method introduced by Wang and coworkers was adopted for the synthesis of the colloidal Pt nanoparticles [26,29]. 50 mL Ethylene glycol solution of NaOH (0.50 M) was mixed with 50 mL ethylene glycol solution of $H_2PtCl_6 \cdot 6H_2O$ (containing 1.00 g (1.93 mmol) of $H_2PtCl_6 \cdot 6H_2O$) with stirring to obtain a transparent yellow platinum hydroxide or oxide colloidal solution. This solution was then heated at 160 °C for 3 h with an N_2 flow to protect the reaction system. A transparent dark-brown homogeneous colloidal solution of Pt metal nanoparticles was obtained without any precipitate.

2.3. Preparation of alumina-supported platinum nanoparticle catalyst

1.00 g Alumina (Al_2O_3) was mixed with the required amount of the above obtained colloidal Pt nanoparticle dispersion in a 50-mL flask, and then the same volume of water was slowly dropped into the mixed dispersion under stirring. The dispersion was kept stirring for 24 h at ambient temperature. After filtration, the solid was washed with deionized water for several times until no chlorine ion was detected, as confirmed by the $AgNO_3$ test. The solid was then dried at 323 K under vacuum for 12 h to give the Al_2O_3-supported Pt nanoparticle catalyst, Pt/Al_2O_3. The content of Pt was 0.44 wt% determined by inductively coupled plasma spectrometry (ICP).

2.4. Selective hydrogenation of o-CNB without solvent

Hydrogenation of *o*-CNB was carried out in a 100 mL stainless steel autoclave with a Teflon tube to avoid metal contamination. The typical reaction condition was to add 5.00 g *o*-CNB and 1.00 g Pt/Al_2O_3 into the autoclave and the reactor was then sealed and flushed with H_2 three times to remove the air. The reactor was heated to 50 °C and H_2 gas was then introduced up to the desired pressure (e.g., 1.0 MPa). The solvent-free hydrogenation reaction was conducted with external magnetic stirring. The H_2 pressure was kept constant by replenishing H_2 as the reaction proceeded. The resulting products were firstly centrifuged to separate the catalyst, and then were analyzed by gas chromatography equipped with a FID detector and a DC-710 column. In some experiments the GC internal standard (0.100 g dodecanol) was directly mixed with *o*-CNB. It was found that the products and the reactant were well balanced in mass.

2.5. Characterization

XRD patterns were recorded with a Rigaku Dmax 2500 diffractometer with Cu radiation at 40 kV and 300 mA. Element analyses of the supported Pt catalysts were carried out on the ULTIMA ICP (France JY Inc.). The XPS spectra were obtained with an ES-CALAB 220I-XL-VG photoelectron spectrometer using monochromatic Mg $K\alpha$ X-ray of 1253.6 eV. All binding energy values were referred to carbon (C_{1s}=285.0 eV). Transmission electron microscopy (TEM) photographs were taken with a JEM-2100 electron microscope. Specimens were prepared by placing a drop of an ethanol dispersion of the catalyst on a copper grid covered with a perforated carbon film and then evaporating the solvent. The nanoparticle sizes were measured from a few randomly selected areas of the enlarged TEM photographs. The average particle size and the particle size distribution histogram were calculated based on the measurements of 300 − 500 individual nanoparticles.

The activity of the nanocatalyst was expressed in the average reaction rate r_a ($mol_{o\text{-CNB}}\ mol_{metal}^{-1}\ h^{-1}$):

$$r_a = n_{o-CNB}/(n_{metal}t),$$

where $n_{o\text{-CNB}}$ was the number of moles of *o*-CNB involved in the conversion reaction, n_{metal} was the total number of metal atoms in the catalysts (mole), and t was the reaction time (h).

3. Results and discussion

3.1. Preparation of the Pt/Al_2O_3 nanocatalyst

Traditional supported catalysts made by wet impregnation are often not easy to control the particle size and the size distribution. Therefore, a series of attempts have been made to immobilize preformed colloidal metal nanoparticles with controllable size and size distribution on supports [26–29]. But most of the immobilized nanoparticles exhibited lower activity comparing to their free

moving colloidal nanoparticles. Yu et al. found that if the protecting ligands used for colloidal nanoparticles were thoroughly removed, the immobilized nanoparticle catalysts could exhibit higher activity and selectivity, because the nanoparticles got back more available active sites by removing the protecting ligands [28,30,31]. Thus, the ethylene glycol reduction method was chosen to make small Pt nanoparticles so that they can be easier to be immobilized on support and expose the active sites for catalysis [26,29].

Representative TEM images and corresponding histograms are shown in Fig. 1 and the elemental analysis by EDX is shown in Fig. 2. From Fig. 1a, we can see that highly dispersed Pt colloidal nanoparticles formed. The colloidal Pt nanoparticles were made according to the literature to get an average particle size of 2.24 nm, with 15% size distribution (Fig. 1a and b). These nanoparticles do not have small molecular or polymeric stabilizing agents so that they are easier to be immobilized [26,29]. Fig. 1c and d shows the particle size (2.21 nm in average) and size distribution (16%) of the as-prepared Pt/Al_2O_3 nanocatalyst. It can be seen that there is no obvious difference before and after immobilization. In other words, the Pt/Al_2O_3 catalyst has controlled small size and narrow size distribution coming from its colloidal nanoparticle precursor.

Alumina (Al_2O_3) is selected to be the support for their extensive use as catalyst support in industrial hydrogenation. It is well known that the catalyst supports play an important role in the catalytic activity [32]. The catalytic performance of alumina-supported catalysts is largely dependent on the textural properties of the alumina supports [33]. X-ray diffraction (XRD) patterns of the Al_2O_3 support itself and the Pt/Al_2O_3 nanocatalysts showed

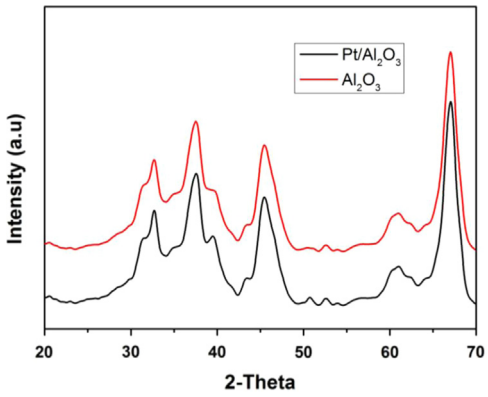

Fig. 2. XRD patterns of Al_2O_3 and Pt/Al_2O_3.

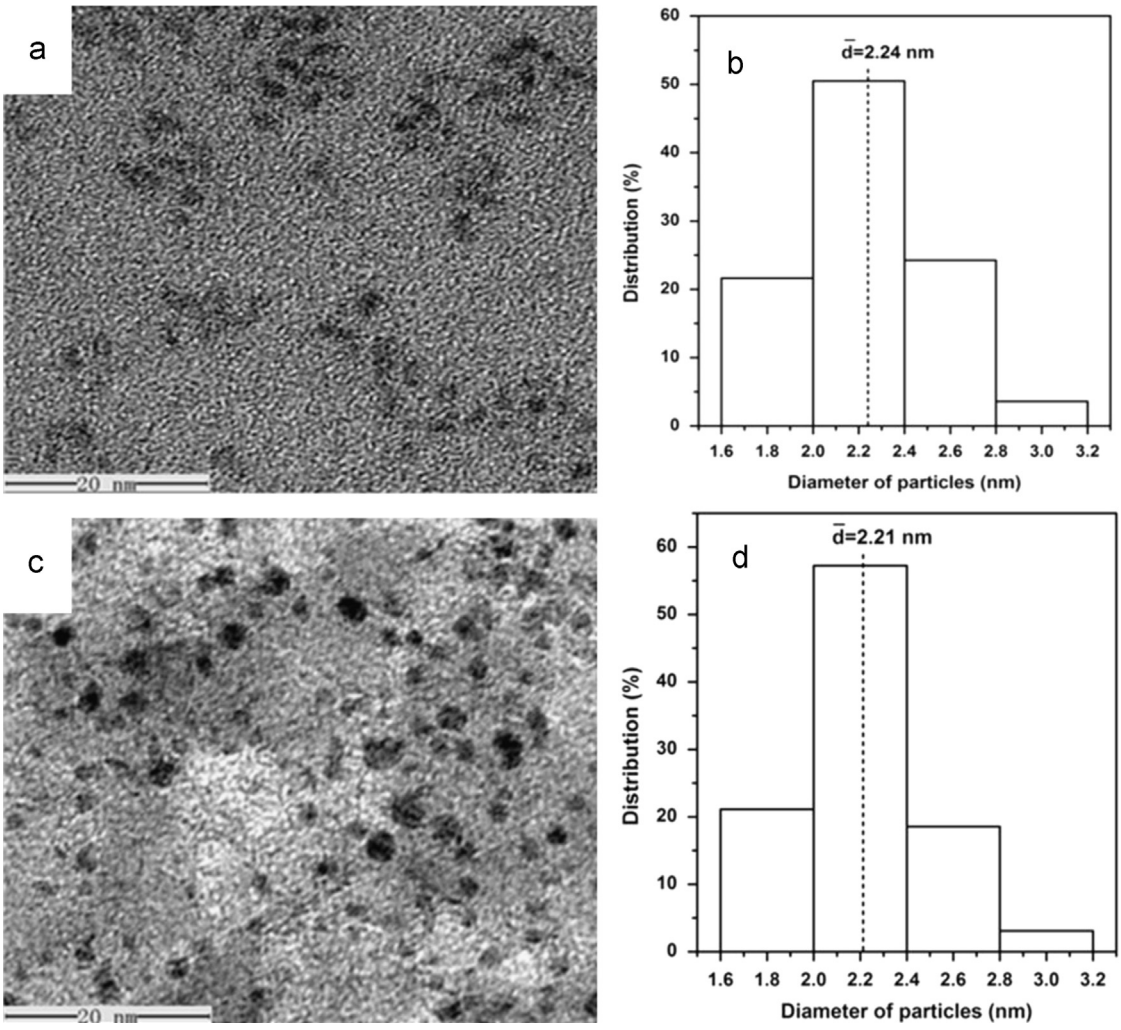

Fig. 1. TEM photographs and size distribution histograms of colloidal Pt nanoparticles (a, b) and the immobilized Pt nanoparticles on Al_2O_3 (c, d).

very similar profiles, and almost all of the diffraction peaks were attributed to Al_2O_3 (Fig. 2). No characteristic diffraction peaks ascribed to Pt species were detected due to the low content of Pt (0.44 wt%) in the whole mixture. This also indicated that these particles were dispersed so well that could not produce detectable diffraction signals (i.e., no large particles. See Fig. 1) [34]. The diffraction patterns of the used catalyst remained unchanged, indicating the high stability of Al_2O_3 under the reaction condition.

Energy dispersive spectroscopy (EDS) clearly showed that the catalyst was composed of O, Al, Pt (Cu was from the copper grid; Fig. 3 left). X-ray photoelectron spectrum (XPS) also revealed that the binding energy of Pt $4f_{7/2}$ was exactly the same as the literature value (70.9 eV) [35,36], indicating the metallic state of Pt nanoparticles on Al_2O_3 surface (Fig. 3 right).

3.2. Selective hydrogenation of o-CNB without solvent

The composition change during the hydrogenation of *o*-CNB over Pt/Al_2O_3 was analyzed as a function of reaction time. The evolution of the detectable compounds measured by GC is shown in Fig. 4. The desired product *o*-CAN increased monotonously with reaction time, 80.8% selectivity to *o*-CAN was obtained at 99.6% conversion of *o*-CNB. Aniline (AN) was the main by-product and reached 18.8% at 75 min when *o*-CNB was almost exhausted. It continued to increase after that. This means that the dechlorination happens after N═O bond is completely reduced to $-NH_2$. In addition to AN, trace amount of nitrobenzene (NB) was found, but no other products were detected.

Reaction conditions are known to influence the hydrogenation rate and the selectivity in the hydrogenation of halonitrobenzenes over Pt-based catalysts [9,37]. Wang and coworkers [9] reported that in the hydrogenation of *o*-iodonitrobenzene over a partially reduced $Pt/\gamma\text{-}Fe_2O_3$ nanocomposite catalyst, the hydrogenation rate reached a maximum value with an optimum temperature about 40 °C; when the temperature was higher, the hydrogenation rate decreased significantly, and the selectivity declined slightly. In this work the catalytic reaction results with different temperatures (Nos. 1–4) and pressures (Nos. 2, 5–7) are summarized in Table 1. The results indicated that the activity increased and the selectivity did not change much when the temperature increased. These are understandable that higher temperatures can lead to faster reactions because the increased number of activated molecules will increase the effective collision frequency. However, it was noted that the activity increased a lot when the temperature increased from 40 °C to 50 °C, and the activity did not change much when the temperature further increased from 50 °C to 60 °C. This is due to the melting point of *o*-CNB, which is 33–36 °C. It was very viscous at 40 °C without solvent, which obviously reduced the mass transportation a lot. So the first 10° temperature change made great improvement in mass transfer, and the second 10° made relative less improvement in mass transfer.

When the H_2 pressure is low, it is expected to have a slow reaction (No. 5). Similarly, a higher pressure should lead to a faster reaction. Wang et al. found that the hydrogenation rate of *o*-CNB over a $Pt/\gamma\text{-}Fe_2O_3$ nanocomposite catalyst was 34 times higher when the H_2 pressure changed from 0.1 to 4 MPa at 60 °C and no obvious loss of catalytic selectivity was observed [37]. One *o*-CNB molecule needs three H_2 molecules to become one *o*-CAN molecule, so increasing the H_2 pressure can greatly escalate the overall reaction activity.

Some articles [38–40] reported that in the hydrogenation of some organic substrates the added metal cations in the colloidal metal catalyst systems could obviously influence both the activity and the selectivity. For example, the use of metal cations can not only increase the reaction rate but also increase the selectivity in the hydrogenation of chloronitrobenzene [38],

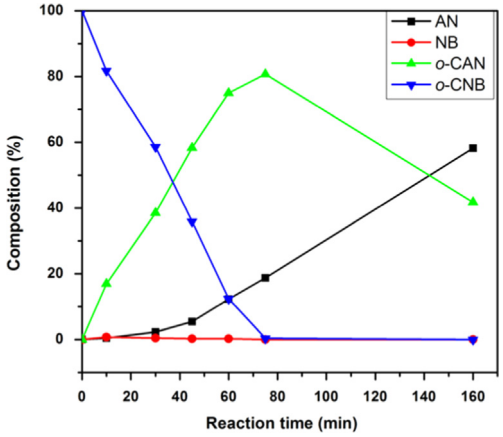

Fig. 4. Composition changes during the catalytic hydrogenation of *o*-CNB (AN═aniline, NB═nitrobenzene).

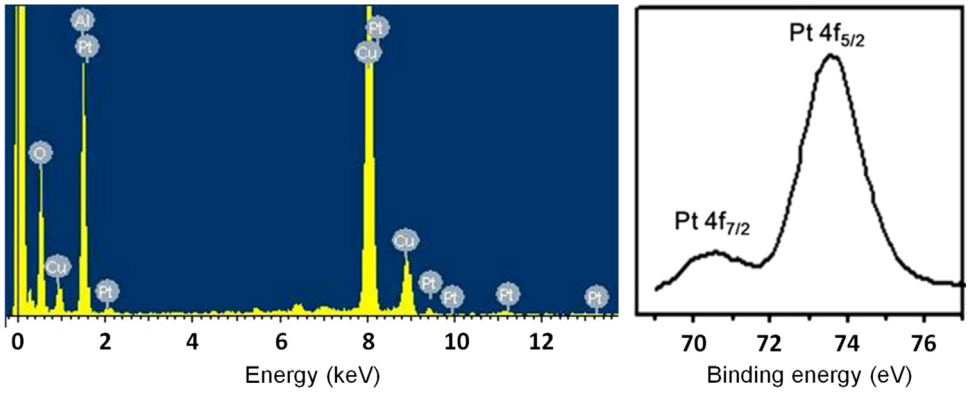

Fig. 3. EDS (left) and XPS (right) characterizations of Pt/Al_2O_3 catalyst.

Table 1
Catalytic hydrogenation of *o*-CNB under different reaction conditions

No.	Quantity of Pt/Al_2O_3 (g)	H_2 pressure (MPa)	Temperature (°C)	Conversion of *o*-CNB (%)	Reaction rate r_a ($mol_{o\text{-CNB}}\ mol^{-1}_{metal}\ h^{-1}$)	Selectivity (%)		
						o-CAN	AN	NB
1	1.00	1.0	40	99.37	493	83.90	15.66	0.44
2	1.00	1.0	50	99.05	1115	84.68	15.32	0.00
3	1.00	1.0	60	98.19	1219	88.49	11.34	0.16
4	1.00	1.0	70	97.79	1314	82.94	17.06	0.00
5	1.00	0.6	50	98.11	652	88.78	11.01	0.21
6	1.00	2.0	50	98.52	1230	88.38	11.31	0.31
7	1.00	3.0	50	100	1749	86.94	13.06	0.00

Note: r_a=the average reaction rate ($mol_{o\text{-CNB}}\ mol^{-1}_{metal}\ h^{-1}$) at the specified conversion, AN=aniline, NB=nitrobenzene.

Table 2
Catalytic hydrogenation of *o*-CNB Pt/Al_2O_3–MCl*x* system.

Catalytic system	Conversion of *o*-CNB (%)	Reaction rate r_a ($mol_{o\text{-CNB}}\ mol^{-1}_{metal}\ h^{-1}$)	Selectivity (%)		
			o-CAN	AN	NB
Pt/Al_2O_3	99.05	1115	84.68	15.32	0.00
Pt/Al_2O_3–Fe^{3+}	99.16	1195	92.63	7.36	0.01
Pt/Al_2O_3–Co^{2+}	100	1034	98.80	1.20	0.00
Pt/Al_2O_3–Ni^{2+}	99.38	1040	93.58	6.42	0.00
Pt/Al_2O_3–Sn^{4+}	99.95	1034	99.79	0.21	0.00
Pt/Al_2O_3–Zn^{2+}	96.04	1108	92.15	7.85	0.00

Reaction conditions: 1.00 g Pt/Al_2O_3, Pt: 2.255×10^{-5} mol, the molar ratio of the modifier to Pt was 1:1, 5.00 g *o*-CNB, P_{H2}=1.0 MPa, T=323 K, AN=aniline, NB=nitrobenzene. r_a=the average reaction rate ($mol_{o\text{-CNB}}\ mol^{-1}_{metal}\ h^{-1}$) at the specified conversion.

cinnamaldehyde [39,40], crotonaldehyde [40], and citronellal [28] over polymer-stabilized Pt colloids. Whereas, some metal cations introduced to the polymer-stabilized Ru colloids improved the activity and the selectivity remained unchanged [41]. Therefore, we also investigated the metal cation effect in our Pt/Al_2O_3 system, and the results are summarized in Table 2.

Metal cations adsorbed on colloidal particles modify the particle's surface electronic structures; as a result alter their catalytic performances [42]. It can be seen in Table 2 that the addition of metal cations influences largely on the selectivity. For the selective hydrogenation of N=O double bonds, Sn^{4+} is the best, followed by Co^{2+}, Ni^{2+}, and Fe^{3+}. Yang et al. [43] found that the competitive coordination of Ni^{2+} with amino group of the products caused the product *o*-CAN to be desorbed from the platinum surface easier, so that the dechlorination was suppressed to a larger extent in the PVP-Pt-Ni^{2+} system. It can be seen here that the VIII group metal caions, such as Fe^{3+}, Co^{2+}, and Ni^{2+}, can improve the selectivity in different degrees. It is reported that Sn^{4+} and Zn^{2+} are poisonous to the catalyst in the hydrogenation of *o*-CNB to *o*-CAN over polymer-stabilized Pt colloids [43]. However, it is surprising to notice that both Sn^{4+} and Zn^{2+} acted as promoters in this system. Wang et al. [44] reported that a Ru/SnO_2 nanocomposite catalyst exhibited excellent catalytic properties for the chloronitrobenzene hydrogenation reaction; an *o*-CAN selectivity over 99.9% at a substrate conversion of 100% was obtained. This selectivity was higher than that of the PVP-Ru colloidal catalyst which had the same Ru nanoparticles. Our work [45] also showed 99.5% selectivity to *o*-CAN at ~100% conversion was achieved for selective hydrogenation of *o*-CNB to *o*-CAN over a Pt–Ru/SnO_2 nanocatalyst. However, the selectivity to *o*-CAN was only 79.80% at the complete conversion of *o*-CNB over the PVP-Pt-Ru colloid catalyst with the same Pt–Ru alloyed nanoparticles. Apparently a similar synergic effect happened in our case with Sn^{4+} (and probably Zn^{2+}), which may be due to the electronic interaction between Pt particles and Sn^{4+} and Zn^{2+} cations.

We further tested the stability of the as-prepared Pt/Al_2O_3 catalyst. The results indicated that the activity dropped a little after reusing it three times. The activity of the recovered catalyst was 986 $mol_{o\text{-CNB}}\ mol^{-1}_{metal}\ h^{-1}$, which was 11% lower than that of the fresh nanocatalyst (the selectivity to *o*-CAN did not change). TEM photograph of the used catalyst is shown in Fig. 5. It can be seen that the particles on the surface of the Al_2O_3 support remained the same size and size distribution. However, the content of Pt was 0.39 wt% detected by ICP, which was lower than that of the fresh Pt/Al_2O_3 catalyst (0.44 wt%). The 11.4% loss of the active metal (Pt) corresponded directly to the drop of the activity. Further study on improving the stability is undergoing in the lab.

In order to compare the as-prepared nanocatalyst with traditional catalysts, we made a Pt/Al_2O_3 catalyst by impregnation (Pt/Al_2O_3-imp). The activity and the selectivity to *o*-CAN were 325 $mol_{o\text{-CNB}}\ mol^{-1}_{metal}\ h^{-1}$ and 91.1%, respectively. The results demonstrated that the Pt/Al_2O_3 nanocatalyst was more active than the classically prepared catalyst, because

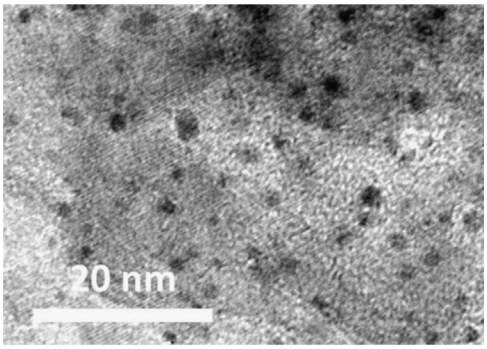

Fig. 5. TEM photograph of the Pt/Al_2O_3 catalyst after 3 times reactions.

the size and size distribution of Pt particles were much smaller and narrower than those in the Pt/Al_2O_3-imp catalyst. Even after being reused for three times, the activity of the Pt/Al_2O_3 nanocatalyst was still much higher than that of Pt/Al_2O_3-imp catalyst (986 to 325 $mol_{o\text{-CNB}}\ mol_{metal}^{-1}\ h^{-1}$).

4. Conclusions

The catalytic activity of Pt/Al_2O_3 nanocatalyst depended on hydrogen pressure and temperature, but temperature and pressure had no significant effect on the selectivity. The modification of metal cations could improve the activity in various degrees while maintained the high selectivity.

Acknowledgments

This work was financially supported by the National Natural Science Foundation of China (21301103), the Taishan Scholarship, the Shandong Natural Science Foundation (ZR2012FZ007), and the Shandong Province High Education Research and Development Program (J13LA08).

References

[1] D.C. Dittmer, Chem. Ind. 19 (1997) 779–784.
[2] F. Toda, Acc. Chem. Res. 28 (1995) 480–486.
[3] O. D'Alessandro, Á.G. Sathicq, J.E. Sambeth, H.J. Thomas, G. P. Romanelli, Catal. Commun. 60 (2015) 65–69.
[4] P. Upadhyay, V. Srivastava, RSC Adv. 5 (2015) 740–745.
[5] V.R. Choudhary, D.K. Dumbre, Catal. Commun. 13 (2011) 82–86.
[6] W. Zhang, X. Dong, W. Zhao, Org. Lett. 13 (2011) 5386–5389.
[7] X.D. Wang, M.H. Liang, J.L. Zhang, Y. Wang, Curr. Org. Chem. 11 (2007) 299–314.
[8] O. Verho, K.P. Gustafson, A. Nagendiran, C.W. Tai, J.E. Bäckvall, ChemCatChem 6 (2014) 3153–3159.
[9] M. Liang, X. Wang, H. Liu, H. Liu, Y. Wang, J. Catal. 255 (2008) 335–342.
[10] C. Evangelisti, L.A. Aronica, M. Botavina, G. Martra, C. Battocchio, G. Polzonetti, J. Mol. Catal. A: Chem. 366 (2013) 288–293.
[11] M.H. Liu, W.Y. Yu, H.F. Liu, J. Mol. Catal. A: Chem. 138 (1999) 295–303.
[12] T. Lu, H. Wei, X. Yang, J. Li, X. Wang, T. Zhang, Langmuir 31 (2015) 90–95.
[13] K. Shimizu, Y. Miyamoto, A. Satsuma, J. Catal. 270 (2010) 86–94.
[14] K.I. Shimizu, Y. Miyamoto, T. Kawasaki, T. Tanji, Y. Tai, A. Satsuma, J. Phys. Chem. C 113 (2009) 17803–17810.
[15] V. Kratky, M. Kralik, M. Mecarova, M. Stolcova, L. Zalibera, M. Hronec, Appl. Catal. A: Gen. 235 (2002) 225–231.
[16] A. Yarulin, I. Yuranov, F. Cárdenas-Lizana, D.T. Alexander, L. Kiwi-Minsker, Appl. Catal. A: Gen. 478 (2014) 186–193.
[17] J.P. Stassi, P.D. Zgolicz, S.R. de Miguel, O.A. Scelza, J. Catal. 306 (2013) 11–29.
[18] B. Coq, A. Tijani, F. Figueras, J. Mol. Catal. 68 (1991) 331–345.
[19] Y. Hartadi, D. Widmann, R.J. Behm, ChemSusChem 8 (2015) 456–465.
[20] R.S. Suppino, R. Landers, A.J.G. Cobo, Appl. Catal. A: Gen. 452 (2013) 9–16.
[21] K.V.R. Chary, D. Naresh, V. Vishwanathan, M. Sadakane, W. Ueda, Catal. Commun. 8 (2007) 471–477.
[22] P. Panagiotopoulou, A. Christodoulakis, D.I. Kondarides, S. Boghosian, J. Catal. 240 (2006) 114–125.
[23] D. Lee, G.S. Jung, H.C. Lee, J.S. Lee, Catal. Today 111 (2006) 373–378.
[24] A. Miyazaki, I. Balint, K. Aika, Y. Nakano, J. Catal. 204 (2001) 364–371.
[25] J.M. Nadgeri, M.M. Telkar, C.V. Rode, Catal. Commun. 9 (2008) 441–446.
[26] Y. Wang, J.L. Zhang, X.D. Wang, J.W. Ren, B.J. Zuo, Y.Q. Tang, Top. Catal. 35 (2005) 35–41.
[27] Q. Wang, H.F. Liu, H.G. Wang, J. Colloid Interface Sci. 190 (1997) 380–386.
[28] W.Y. Yu, M.H. Liu, H.F. Liu, X.H. An, Z.J. Liu, X.M. Ma, J. Mol. Catal. A: Chem. 142 (1999) 201–211.
[29] Y. Wang, J.W. Ren, K. Deng, L.L. Gui, Y.Q. Tang, Chem. Mater. 12 (2000) 1622–1627.
[30] W.Y. Yu, H.F. Liu, X.H. An, J. Mol. Catal. A: Chem. 129 (1998) L9–L13.
[31] W.Y. Yu, H.F. Liu, X.H. An, X.M. Ma, Z.J. Liu, L. Qiang, J. Mol. Catal. A: Chem. 147 (1999) 73–81.
[32] C. Evangelisti, L.A. Aronica, M. Botavina, G. Martra, C. Battocchio, G. Polzonetti, J. Mol. Catal. A: Chem. 366 (2013) 288–293.
[33] S. Komhom, O. Mekasuwandumrong, P. Praserthdam, J. Panpranot, Catal. Commun. 10 (2008) 86–91.
[34] X.L. Yang, W.Q. Zhang, C.G. Xia, X.M. Xiong, X.Y. Mu, B. Hu, Catal. Commun. 11 (2010) 867–870.
[35] W.Y. Yu, M.H. Liu, H.F. Liu, X.M. Ma, Z.J. Liu, J. Colloid Interface Sci. 208 (1998) 439–444.
[36] M.H. Liu, J. Zhang, J.Q. Liu, W.W. Yu, J. Catal. 278 (2011) 1–7.
[37] J.L. Zhang, Y. Wang, H. Ji, Y.G. Wei, N.Z. Wu, B.J. Zuo, Q.L. Wang, J. Catal. 229 (2005) 114–118.
[38] X.L. Yang, H.F. Liu, Appl. Catal. A. Gen. 164 (1997) 197–203.
[39] W.Y. Yu, H.F. Liu, Q. Tao, Chem. Commun. 15 (1996) 1773–1774.
[40] W.Y. Yu, H.F. Liu, M.H. Liu, Q. Tao, J. Mol. Catal. A: Chem. 138 (1999) 273–286.
[41] M.H. Liu, W.Y. Yu, H.F. Liu, J. Mol. Catal. A: Chem. 138 (1999) 295–303.
[42] W.W. Yu, H.F. Liu, J. Mol. Catal. A: Chem. 243 (2006) 120–141.
[43] X. Yang, H. Liu, Appl. Catal. A: Gen. 164 (1997) 197–203.
[44] B. Zuo, Y. Wang, Q. Wang, J. Zhang, N. Wu, L. Peng, L. Gui, X. Wang, R. Wang, D. Yu, J. Catal. 222 (2004) 493–498.
[45] M.H. Liu, Q. Bai, H.L. Xiao, Y.Y. Liu, J. Zhao, W.W. Yu, Chem. Eng. J. 232 (2013) 89–95.